

# Efficiency-determined method for thermal neutron detection with inorganic scintillator

FU Zaiwei<sup>1,\*</sup> HENG Yuekun<sup>2,\*</sup> GU Shenjie<sup>1</sup> TIAN Lin<sup>1</sup>

<sup>1</sup>Shanghai Nuclear Engineering Research & Design Institute, Shanghai 200233, China

<sup>2</sup>Institute of High Energy Physics, Chinese Academy of Sciences, Beijing 100049, China

**Abstract** Because of <sup>3</sup>He shortage, scintillator is a promising alternative choice for neutron detection in the field of thermal neutron scattering and imaging. Also, the neutron detection efficiency is difficult to be determined. In this paper, the efficiency for thermal neutron detection is presented by inorganic scintillator using probability principles, supposed that the material of scintillator is uniform in element distribution, and that attenuation length of scintillation light is longer than that of its thickness in the scintillator. The efficiencies for two pieces of lithium glass are determined by this method, indicating the method is useful for determining efficiency of thermal neutron detections.

**Key words** Detection efficiency, Inorganic scintillator, Thermal neutron, Lithium

## 1 Introduction

Along with building more intense reactor and spallation neutron sources<sup>[1,2]</sup>, thermal neutrons with high flux are produced for neutron scattering and imaging in material science and other applications<sup>[3-5]</sup>, many neutron detectors with high quality are increasingly developed. Thermal neutron means that its speed is reduced to below 1 eV, where it has approximately the same average kinetic energy of ~0.025 eV at 20°C as the atoms or molecules in the medium, and it is undergoing elastic scattering. Neutron detectors commonly use <sup>3</sup>He gas, but the <sup>3</sup>He shortage worldwide forces people to look for the future alternative ways, and inorganic scintillator detector is promising, especially doped with <sup>6</sup>Li, <sup>10</sup>B, or <sup>155,157</sup>Gd.

Determining the detection efficiency is tough for the scintillator detector due to the following factors. Firstly, it is hard to find an established standard neutron source, and to subtract the accompanied gamma rays background from the neutron signals. Secondly, neutrons are usually not monoenergetic, the detection efficiency varies with the neutron energy,

especially at the energy of less than 5 MeV<sup>[6]</sup>. Finally, the efficiency often depends on the detector properties and the counting geometry in experiments.

Though difficulties exist on efficiency determination, there are multiple reasons to know efficiency in the neutron detection since it is related to the experiment designing, detector and engineering construction, and so on.

The Monte Carlo (MC) method can be used to get neutron detection efficiency<sup>[7]</sup>. Taking into account of the factors of neutron energy, electronic threshold, and scintillator shape, the MC simulation may be more perfect. But simulation results are sensitive to the basic input data because there are uncertain ties for disturbing<sup>[8]</sup>. Alternatively, neutron detection efficiency ( $\varepsilon_A$ ) can be calculated using an analytical expression<sup>[9]</sup> (Eq.(1)).

$$\varepsilon_A = 1 - e^{-n\sigma l} \quad (1)$$

here,  $n$  is number density of material atoms,  $\sigma$  is neutron capture cross section, and  $l$  is the thickness of scintillator. For lithium glass, Eq.(1) can be used to calculate the 5% accuracy efficiency below 100 eV<sup>[10]</sup>.

Above way may provide the useful information on neutron detection efficiency, but cannot fulfill the

Supported by the National Natural Science Foundation of China (Grant No.10875140)

\* Corresponding author. E-mail address: fuzaiwei@snerdi.com.cn, hengyk@ihep.ac.cn

Received date: 2012-10-25

requirements of experiment, and engineering design and construction. In many cases, the efficiency for the neutron detector should exactly be known by employing experiments.

In experiment, relative method<sup>[11]</sup> can be used to simply determine neutron flux, but the measured efficiency often depends on reference detector which should be studied carefully. In this paper, the efficiency determination for thermal neutron detection is presented and discussed by inorganic scintillators. The efficiencies of two lithium glass are tested and calculated. Their theoretical and experimental efficiencies are compared.

## 2 Efficiency model analysis

### 2.1 Efficiency definition

Neutron detection efficiency is usually subdivided into the absolute and intrinsic efficiency. The absolute efficiency ( $\varepsilon_a$ ) is defined as

$$\varepsilon_a = N/N_s \quad (2)$$

here,  $N$  is the number of neutron pulses recorded by detector, and  $N_s$  is the number of neutrons emitted by neutron source. Because the  $\varepsilon_a$  depends on both the detector properties and the geometric arrangement of source/detector, it is difficult to be tested.

The intrinsic efficiency ( $\varepsilon_i$ ) is defined as

$$\varepsilon_i = N/N_d \quad (3)$$

here,  $N$  is the same as above,  $N_d$  is the number of neutron incidents on detector. Supposed that the solid angle of the detector subtended to point neutron source is  $\Omega$ , the  $\varepsilon_a$  equals to  $\Omega \times \varepsilon_i / 4\pi$ . If the detector covers a point source in a solid angle of  $4\pi$ , the same result can be obtained by Eqs.(2) and (3). Thus, it is convenient to scale the absolute efficiency by using intrinsic efficiency. The intrinsic efficiency can be described in the following section unless additional instruction.

Because it is difficult to determine the absolute and intrinsic efficiency, the relative efficiency ( $\varepsilon_r$ ) is usually used and defined as

$$\varepsilon_r = N \times \varepsilon_{ref} / N_{ref} \quad (4)$$

here  $N_{ref}$  is the counts recorded by the reference detectors, and  $\varepsilon_{ref}$  is its detection efficiency.

### 2.2 Efficiency-determined method

Neutron as neutral particle travels in straight line, and

deviates from its path when actually colliding with another due to scattering into a new direction or absorption. Table 1 shows the total cross sections of thermal neutron interaction with some elements (referenced from ENDF/B-VII.0). The elements are major compositions for some inorganic scintillators, and the cross sections of thermal neutron with host elements in most of inorganic scintillator are small and even ignorable. Consequently, the energy loss in the thermal range is very small. In another aspect, their maximum energy loss at a collision, which is easily calculated, is no more than 2%. So, the energy loss caused by the host elements is ignorable. Hence the two destinations for incident neutrons in the scintillator are either escaped out or captured by the neutron sensitive elements like  ${}^6\text{Li}$ ,  ${}^{10}\text{B}$  and  ${}^{155,157}\text{Gd}$ .

**Table 1** Total cross sections in barns for thermal neutron of some elements

Elements	$E_1$ /eV	$\sigma(E_1)$	$\sigma(0.0253 \text{ eV})$
Na	1.010	3.277	3.919
I	1.039	4.653	9.878
Cs	1.053	9.518	32.977
Zn*	1.058	16.333	72.202
S	1.024	1.054	1.514
Si	1.024	1.985	2.160
O	1.024	3.858	3.973
Ca	1.010	3.088	3.470

\*Referenced from ENDF/B-VII.1

For inorganic scintillator detector based on nuclear reaction of neutron sensitive elements, like  ${}^6\text{Li}$ ,  ${}^{10}\text{B}$  and  ${}^{155,157}\text{Gd}$ , the neutron can penetrate into the scintillator materials directly until the nuclear interaction occurs. Once a photomultiplier (PMT) coupled with the scintillator can detect the scintillating light caused by the nuclear reaction, it will record an effective pulse. Experimentally, the detection efficiency of electronic system for a scintillation detector can be realized nearly 100% by choosing the suitable PMT and its threshold setup.

Supposed that the element distribution in the thick scintillator ( $L$ ) is uniform where  $L$  can be divided into equal thicknesses ( $L_n$ ), we have the equal detection efficiency ( $L/n$ ). Also, the thick scintillator can be considered to consist of these thin scintillators with perfect junctions, which cannot affect their uniformity and optical properties. Fig.1 depicts a thick

scintillator. Dashed lines are  $n$ -th partition divisions of  $Scin\_i$  ( $i=1,2,\dots,n$ ), and identical for each other.

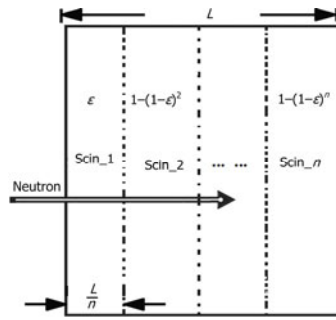


**Fig.1** Schematic diagram of a square thick scintillator with the thickness ( $L$ ).

$N_1$  is defined as the neutron numbers detected by the  $Scin\_1$ ; and  $N_n$ , the total tiles of  $Scin\_1$  to  $Scin\_n$ . The detection efficiency of the thick scintillator is defined as  $\varepsilon_t$ . Then, its detection efficiency for the  $Scin\_1$  is

$$\varepsilon = N_1 / N_d \quad (5)$$

And  $\varepsilon_t$  is

$$\varepsilon_t = N_n / N_d \quad (6)$$

If the attenuation length of scintillation light is longer than  $L$ ,  $\varepsilon_t$  is expressed by using  $\varepsilon$  as the following analysis. For an incident neutron, the detected probability is  $\varepsilon$  in the  $Scin\_1$ , and its undetected probability is  $1-\varepsilon$ . Since all the tiles for  $Scin\_i$  ( $i=1,2,\dots,n$ ) are identical and the energy loss are ignorable, the undetected probability for the  $Scin\_2$  is  $1-\varepsilon$ , the detected probability of both  $Scin\_1$  and  $Scin\_2$  for the incident neutron becomes  $1-(1-\varepsilon)^2$ . After the neutron passed the  $Scin\_n$ , the detected probability for union tiles of  $Scin\_1$  to  $Scin\_n$  is

$$\varepsilon_t = 1 - (1-\varepsilon)^n \quad (7)$$

From Eqs.(5)–(7), Eq.(8) is obtained.

$$\varepsilon / [1 - (1-\varepsilon)^n] = N_1 / N_n \quad (8)$$

Eq.(8) shows that the scintillator detection efficiencies are obtained by their relative counts. Determining the efficiency of thick scintillator from the thinner scintillator efficiencies is actually the relative efficiency way under unknown any efficiency.

### 3 Lithium glass scintillator efficiencies

The efficiencies of lithium glass are figured out by using above method and compared with theoretical MC calculation.

### 3.1 Glass properties and test setup

The lithium glass compositions are listed in Table 2. The abundance of  ${}^6\text{Li}$  is around 90%, and its mass density is  $2.31 \text{ g/cm}^3$ . Here, the lithium glass of 1-mm and 3-mm thicknesses in 5-cm diameter are adopted. The light yields were measured around 5671 photons per neutron and 3768 photons per MeV gamma rays deposition<sup>[12]</sup>. The 3-mm thick lithium glass can be considered to be comprised of the three 1 mm with perfect junctions, thus the  $n$  in Eq.(8) is equal to 3.

**Table 2** Lithium glass compositions<sup>[8]</sup>

Composition	SiO <sub>2</sub>	Li <sub>2</sub> O	Al <sub>2</sub> O <sub>3</sub>	Ce <sub>2</sub> O <sub>3</sub>
Weight fraction	74.32%	13%	7.52%	5.16%

The test setup is shown in Fig.2. A point neutron source ( ${}^{252}\text{Cf}$ ) with activity of  $5 \times 10^6 \text{ Bq}$  is shielded in a box. The emitted neutrons are thermalized into thermal range and guided out through a channel with a 10-cm diameter, where the thermal neutron emission frequency is around 1–2 Hz/cm<sup>2</sup>. The glass scintillator, greased with silicon oil, is coupled with a PMT (XP2020) with the gain of  $1.2 \times 10^7$ . Tyvek films are used for the packages in order to collect the scintillation light, and the efficiency of whole test system, including that the PMT quantum efficiency, is around 10%. Because the PMT is sensitive to single photon, scintillation lights caused by neutrons can be detected efficiently by the PMT. To shield gamma rays, a lead plate with the 5-cm thickness is fixed in the front of the PMT. In the background test, an additional cadmium plate with the 3-mm thickness is placed between the moderator and lead plate to absorb neutrons.

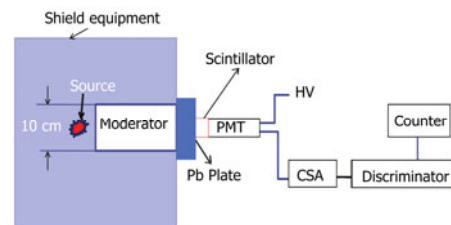


**Fig. 2** Test setup of neutron count rates.

In test, the signal from the PMT is sent into a charge sensitive amplifier (CSA), its signal output is discriminated by a discriminator (Lecroy 623B) and sent into a counter (Caen Mod.N145) to record the counts. The CSA is used mainly for shaping and

amplifying detector signals to avoid the multiple output pulse discriminations and the missed discrimination for a small pulse.

To ensure each signal can be discriminated and recorded by the counter, the threshold of discriminator is selected as low as possible. This is easily realized for the high light output of the glass and the high gain of PMT. Under this condition, the efficiency of this electronic system and the light collection can be considered as around 100%. Thus the efficiency of neutron detector is only determined by the lithium glass contribution.

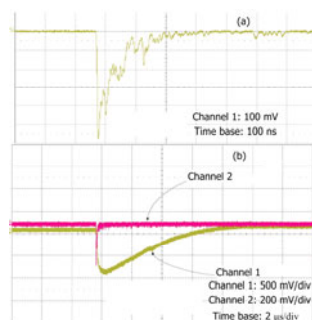


**Fig.3** (a) The original pulse output without amplification, (b) the original pulse and its amplified shape after CSA.

Figure 3(a) shows a neutron original pulse of the PMT output. Because a low threshold can cause multiple discrimination of the same pulse, the CSA is necessary. The channel 1 is the original pulse direct output from PMT; and Channel 2, after the CSA, indicating that the pulse becomes smoother and larger in Fig.3(b) than in Fig.3(a). Consequently, multiple discriminations can be avoided in most cases, and the probability of the missed discriminations decreases. The discriminator, set with a 90-mV threshold, is comparably low according to the pulse height. Though the pulse after CSA is lasting up to 8  $\mu$ s, it enough responds to the neutron flux in this experiment.

### 3.2 Experimental efficiencies

The detection efficiencies are measured by two measurement steps of the background counts, and the total counts of backgrounds and signals. The former is recorded by a cadmium plate between the lead plate and moderator; and the latter, without cadmium plate.

Table 3 shows that the counts of lithium glass with the 1- mm and 3-mm thicknesses are tested by the setup (Fig.2).  $C_a$  and  $C_b$  are the counts without and

with cadmium plate, respectively.  $C_a - C_b$  means the neutron events after background counts are subtracted.

**Table 3** Lithium glass neutron counts in 1400 s

Lithium glass / mm	$C_a$	$C_b$	$C_a - C_b$	$E_{eff}/\%$
1	38719	12445	26274	65.6
3	69412	31010	38402	95.9

From Eq.(8), the  $C_a - C_b$  for the 1-mm and 3-mm lithium glass corresponds to the  $N_1$  and  $N_3$ . Supposed that the efficiency of 1-mm lithium glass is  $\varepsilon$ , an efficiency equation of one variable is

$$\varepsilon/[1-(1-\varepsilon)^3] = 26274/38402 \quad (9)$$

This equation can be solved as that the  $\varepsilon$  equal to 65.6%; and  $1-(1-\varepsilon)^3$ , 95.9%, as listed in Table 3.

### 3.3 Theoretical efficiencies

The nuclear reaction probability of neutron was simulated by  ${}^6\text{Li}$  glass using Geant4. Because the efficiency of electronic system and light collection can be considered as 100% for the efficiency detection, the PMT is ignorable. The lithium glass is placed on the  $x-y$  plane, and its center is superposed with the glass origin. A point beam gun with the 25.3-MeV energy shoots thermal neutrons from the glass origin of (0 mm, 0 mm, 10 mm). The physics list uses the QGSP\_BERT\_HP recommended by Geant4 at low energy range<sup>[13]</sup>. The neutron reaction probabilities of  ${}^6\text{Li}(n,\alpha){}^3\text{H}$  is recorded after 100 000 neutron shots at the two pieces of lithium glass. The captured efficiency approaches the neutron detection efficiencies, as listed in Table 4.

Compared with the simulations, the detection efficiencies are calculated by Eq.(1) That the  $\sigma$  equals to 940 barns is the neutron cross section with the 25.3-MeV energy, as listed in Table 4.

**Table 4** Lithium glass efficiencies from simulation and analytical calculation

Lithium glass / mm	Simulated/%	$\varepsilon_A/\%$
1	67.0	69.0
3	96.2	97.0

The efficiency discrepancies between Tables (3) and (4) may be caused by the following uncertainties. Firstly, Table 3 just described the interaction probabilities of  ${}^6\text{Li}(n,\alpha){}^3\text{H}$ . For a neutron incident, each interaction may not cause absolutely an effective pulse height recorded by the experiment, but the

simulation and analytical calculation can reach these results. Secondly, the efficiencies in Table 4 assumed that all the neutrons are 25.3 MeV, but neutron energies actually distribute around 25.3 MeV after the moderator (Fig.2).

At a given threshold of 555 pC<sup>[12]</sup>, the detection efficiency for the 1-mm lithium glass is 65.2%; and 3 mm, 95.8%, this approaches our results in this paper. In addition, the suppression capability is  $1.8 \times 10^{-3}$  at the 95.8% efficiency. It is said that the presented method is credible in detection efficiency determination of neutron scintillator.

#### 4 Conclusion

An efficiency-determined way of neutron scintillator is presented, and its model is discussed by using probability principle. An application on the efficiencies of two pieces of lithium glass is studied, indicating that the efficiencies are 65.6% for the 1-mm thick lithium glass; and 95.9%, 3 mm, this agrees with the theoretical efficiency.

Based on two assumptions, the elements distribution in the scintillator is uniform, and the attenuation length of scintillation light is longer than the scintillator thickness. If the scintillator is too opaque or thick, the scintillation light generated in the preceding parts would miss detection due to hardly penetrating through all the subsequent material, but the

two assumptions are easy to be realized by material selections for many scintillators in neutron detections.

#### References

- 1 CSNS. <http://csns.dalng.gov.cn/>. [2012-10-25].
- 2 CSNS. <http://neutron-www.kek.jp/>. [2012-10-25]
- 3 Feng Q X, Feng Q K, Takeshi K W. Nucl Sci Tech, 2008, **19**: 282–289.
- 4 Ravisankr R, Eswaran P, Seshaderssan N P, *et al.* Nucl Sci Tech, 2007, **4**: 204–211.
- 5 Komura K, Ahmed N K, EL-Kamel A H, *et al.* Nucl Sci Tech, 2004, **15**: 248–256.
- 6 Jackson W R, Divatia A S, Bonner B E, *et al.* Nucl Instrum Methods, 1967, **55**: 349–357.
- 7 Cub J, Finck E, Gebhardt. K, *et al.* Nucl Instrum Meth A, 1989, **274**: 217–221.
- 8 Cub J, Finck E, Gebhardt. K, *et al.* Nucl Instrum Meth A, 1989, **274**: 217–221.
- 9 Ian S, Anderson, Robert L McGreevy, Hassina Z Bilheux. Neutron Imaging and Applications, NewYork, 2009, Chapter 1: 5–7.
- 10 Dalton A W, Nucl Instrum Meth, 1971, **92**: 221–227.
- 11 Kononov V N, Poletaev E D, Bohovko M V, *et al.* Nucl Instrum Meth A, 1985, **234**: 361–366.
- 12 Fu Z W, Jia R, Heng Y K, *et al.* Chin Phys C, 2012, **36**: 1095–1100. [http://geant4.cern.ch/support/proc\\_mod\\_catalog/physics\\_lists/useCases.shtml](http://geant4.cern.ch/support/proc_mod_catalog/physics_lists/useCases.shtml)